



OPEN

Report of bioerosions and cells in Cainotheriidae (Mammalia, Artiodactyla) from the phosphorites of Quercy (SW France)

Qian Wu^{1,2}✉, Romain Weppe³, Carine Lezin⁴, Yanhong Pan⁵ & Alida M. Bailleul²✉

The phosphorites of the Quercy from SouthWest France are well known for fossils preserved in 3D with phosphatized soft-tissues. Given that phosphatization is known to favor fine cellular preservation, the present study delves into the histological analysis of white and brown bones of Cainotheriidae (Artiodactyla) recently excavated from the DAM1 site near Caylus. Microscopy revealed that the white bones were completely filled with bacterial erosions, while the brown bones showed a pristine histology and intralacunar content resembling fossilized osteocytes in some areas. After decalcification, a brown bone revealed an abundance of blood vessel-like structures, innumerable osteocyte-like structures with canaliculi and a few chondrocyte-like structures, while a white bone revealed only blood vessel-like structures that looked eaten away. All the data combined suggest the brown bones were shielded from bacterial attacks and were filled with fossilized organic matter and original biological structures. The data taken all together do not support that these structures are casts, but indeed original and endogenous cells. This study encourages further histochemical and mineralogical analyses on Quercy fossils and the unique taphonomy of DAM1 to better understand fossilization processes and their impact on the color of bones, the chemistry of skeletal tissues, soft tissues, and cells.

Keywords Quercy, Bacterial erosions, Cells, Bone color, Phosphatization

The “Phosphorites du Quercy” are located in southwest France and consist of plenty of fossiliferous sites from the Paleogene^{1,2}. Since the 19th century, a large number of fossil animals have been excavated from the detrital and phosphatic sediments filled in the karst cavities along with the development of mining activities^{1,2}. These fossils encompass disarticulated vertebrate bone fossils^{3–7}, as well as in some rare cases, amphibians, reptiles and insect fossils with soft tissues preserved in three dimensions (3D)^{2,8–12}, representing a thriving Paleogene fauna¹³.

These Quercy fossils with 3D preserved soft tissues were often referred to as the external casts of “mummies”^{8–10}. However, computerized tomography (CT) later revealed that the skeleton and soft tissue anatomical structures were internally preserved^{8–10}. The external casts were presumed to be made of phosphatic calcium^{2,8,9}, which was confirmed by X-ray diffraction identifying phosphate minerals (i.e., apatite, francolite) in fossil insects¹⁴. The environment of Europe in the Paleogene was similar to a tropical rainforest, with erosion and karstification of Mesozoic bedrocks occurring due to carbon dioxide-enriched water^{15,16}. Sediments rich in clay, quartz, ferruginous oxides and phosphate were accumulated within karstic cavities, where animals fell into karstic sink holes⁵.

¹University of Chinese Academy of Sciences, Beijing, China. ²Key Laboratory of Vertebrate Evolution and Human Origins, Institute of Vertebrate Paleontology and Paleoanthropology, Chinese Academy of Sciences, Beijing, China.

³Institut des Sciences de l’Évolution de Montpellier, Univ Montpellier, CNRS, IRD, Montpellier, France. ⁴Observatoire Midi Pyrénées, Géosciences Environnement Toulouse (GET), UMR 5563, CNRS-CNRS-IRD-Université Toulouse III, 14 Avenue E. Belin, 31400 Toulouse, France. ⁵State Key Laboratory for Mineral Deposits Research, School of Earth Sciences and Engineering, Centre for Research and Education on Biological Evolution and Environment and Frontiers Science Center for Critical Earth Material Cycling, Nanjing University, Nanjing 210093, China. ✉email: wuqian@ivpp.ac.cn; alida.bailleul@ivpp.ac.cn

Phosphatization is an important taphonomic process of exceptional fossil preservation^{17–20}. Notable phosphatized fossils worldwide exhibit preserved cellular or sub-cellular structures, such as the putative embryos of the Neoproterozoic Doushantuo Formation from China^{21–23}, fish muscle fibers of the Mesozoic Santana Formation of Brazil^{24,25}, and the dermal pigment cells of a snake from the Late Miocene Libros Konservat-Lagerstätte from Spain²⁶, emphasizing the importance of studying Quercy's phosphatized fossils for insights into cellular and even subcellular preservation.

The newly excavated site DAM1 dating from the Upper Eocene revealed many Cainotheriidae (Mammalia, Artiodactyla) fossils, notably the species *Paroxaeron valdense*⁷. In this new site, the fossil bones showed different colors, some were white, some were beige and some were brown with a shiny patina (Fig. 1). Some bones also showed all types of shades within the same element (Fig. 1).

Here, we investigated six bones with standard ground-sectioning methods as well as scanning electron microscopy (SEM) paired with Energy Dispersive Spectroscopy (EDS). Additionally, two other bones were decalcified in EDTA (Ethylenediaminetetraacetic acid). For the first time, we report (1) the histological preservation of mammalian skeletons and (2) osteocyte preservation in the Quercy. We also demonstrate a link between bone color and the preservation of original microscopic structures and give some insights on the taphonomic histories of these bones. This study further encourages the comparison of the taphonomic processes, histology, cellular paleontology and chemistry of different fossil sites from the Quercy.

Results

Histology of the white bones

The patella QU-1, femoral head QU-3 and the distal epiphysis of femur QU-6 are white in color. Thin-section slices indicate that the bone tissue in these specimens has undergone extensive modifications (Figs. 2, 5 and 6). Patella QU-1 is made of cancellous bone with many trabeculae (Fig. 2B). The matrix of the cancellous bone tissue shows many dark brown areas with few light areas made of unaltered bone matrix (Fig. 2B–D). The dark brown areas are composed of channels and pores corresponding to Non-Wedl Microscopical Focal Destructions (MFD) resulting from bioerosion^{27,28}. Notably, the spaces between the trabeculae are partially filled with detrital clay (Fig. 2E). The Non-Wedl MFDs are the pores and channels left by bacterial colonies during post-mortem bacterial invasions²⁷. We will refer to them directly as 'bacterial colonies' for readability.

At high magnification under the SEM, we did not see any evidence of fossilized/mineralized bacteria within the pores (Fig. 3). However, the pores did show some fibrous material, possibly representing collagen fibers (Fig. 3). These bacterial colonies are dark grey under the SEM, distinct from the unaltered bone around them. Within the bacterial colonies, osteocyte lacunae are notably absent, whereas the unaltered bone matrix retains some osteocyte lacunae (Fig. 2D, E). This absence of osteocyte lacunae in areas affected by bacterial colonies indicates substantial damage to the bone matrix microstructure. Similar patterns are observed under transmitted light and SEM images of ground section slices of the femoral head QU-3 and the epiphysis of femur QU-6, where bacterial colonies occupy the cancellous bone matrix (Figs. 5B and C and 6C; Fig. S1, S2).

In summary, this histological examination provides detailed insights into the altered structure of the white bones highlighting that they were originally attacked by bacterial colonies, shows the absence of osteocyte lacunae, and shows the impact on both organic and inorganic components of the bone matrix.

Histology of the brown and beige bones

The patella QU-2, femoral head QU-5 and the diaphysis of femur QU-6 are brown in color and the femoral head QU-4 is beige. Unlike the eroded bone matrix observed in QU-1, these bones show a very well-preserved microstructure in their ground section slices (Figs. 4, 5 and 6). The spaces between the trabeculae of cancellous

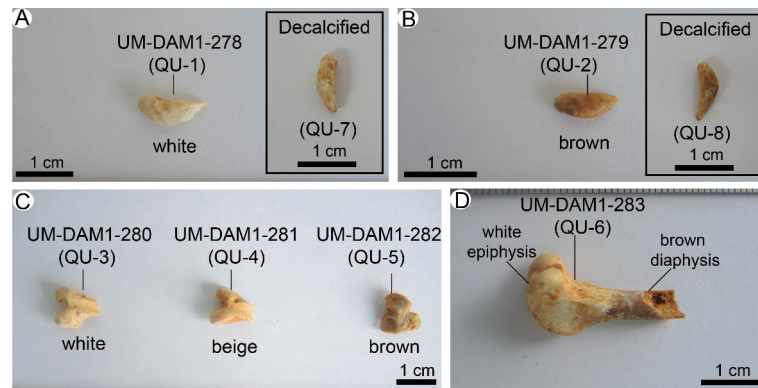


Fig. 1. The eight Cainotheriidae fossils bones from DAM1 analyzed here and showing different colors. The colors range from white to brown. **A**, white patella UM-DAM1-278 (QU-1) and decalcified white patella UN-DAM1-285 (QU-7); **B**, brown patella UM-DAM1-279 (QU-2) and decalcified brown patella UN-DAM1-286 (QU-8); **C**, three unfused distal femoral epiphyses UM-DAM1-280, UM-DAM1-281 and UM-DAM1-282 (QU-3, QU-4 and QU-5) ranging from white to brown; **D**, distal femur UM-DAM1-283 (QU-6) with white epiphysis and a brown diaphysis.

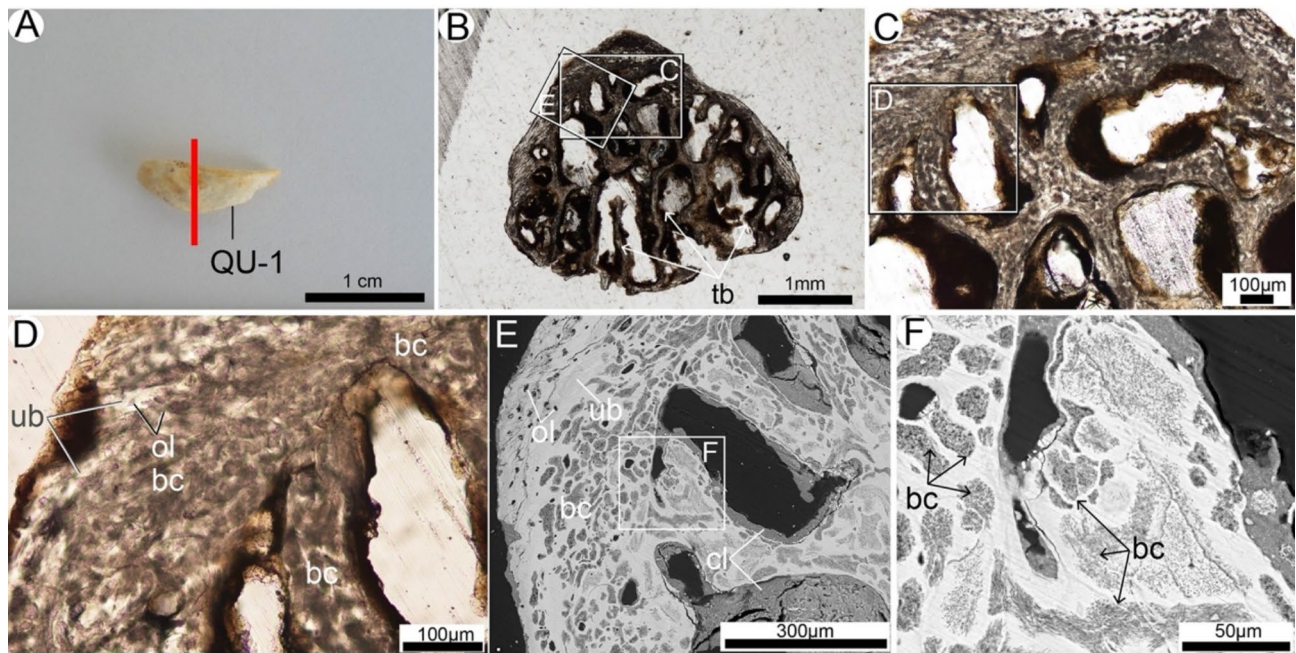


Fig. 2. Histology of the white patella QU-1. **A**, photograph of the patella QU-1 with the red line indicating the direction of the section; **B**, histological cross section of QU-1 under transmitted light and its close-up (**C**) and (**D**), showing the bacterial colonies; **E**, SEM image of the section slice indicated by the box in **B** and its close-up (**F**), showing the bacterial colonies and decrease of bone matrix density. The white patella is heavily attacked by bacterial invasions. Slide is 94 micron thickness. bc, bacterial colony; cl, clay; oc, osteocyte; ol, osteocyte lacuna; tb, trabecula; ub, unaltered bone.

bone in QU-2, QU-4 and QU-5 are filled with clay as in QU-1 and QU-3 (Figs. 4E and H and 5F and I). However, the bone matrix of the trabeculae is notably well preserved, featuring numerous osteocyte lacunae, several osteons, and vascular canals under both transmitted light and SEM observations (Figs. 4 and 5D-I, Fig. S3, S4). Chondrocyte lacunae are organized in line near and perpendicular to the external surface of the bone (Figs. 4F and 5F), as seen in the articular cartilage of extant mammals²⁹. Notably, there are no significant histological differences observed between the beige and brown samples (Fig. 5D-I). The ground section slices of the diaphysis of QU-6 showed good preservation of the bone matrix with significant brown color with some black areas (Fig. 6E). No sign of bioerosion is observed in the corresponding transmitted light and SEM image of the diaphysis of QU-6 (Fig. 6E, F). EDS analysis performed on the same slice showed that these dark areas are made of iron (Fig. 6F). Therefore, these dark areas probably represent a deposition of dark minerals containing iron (i.e., some iron oxides).

In QU-2, some globular intralacunar structures are found in the osteocyte lacunae (Fig. 4C), potentially representing fossilized remnants of original osteocytes or osteoblasts with their nuclei. We attempted to find these intralacunar structures using the SEM directly on the same slide. In the SEM images, some osteocyte lacunae are indeed filled with a material resembling fossil cells (which would align with previous studies^{30–32}) (Fig. 4H-I). In QU-2, 4, 5 and 6 (in all beige and brown areas), similar material was easily found by SEM, while such preservation was not found in the bacterially invaded QU-1 and QU-3 (nor in the bacterially invaded white epiphyses of QU-6).

These intralacunar material filled most of the lacunae in the SEM images, showing a significantly different picture from the dark globule observed under the light microscope (Fig. 4C, I). The dark globule seen under the light microscope is not visible with the SEM, most likely because SEM only shows surface data, whereas standard microscopy shows light shining through a material with a thickness and a depth of field. SEM data indicates the transparent part of the lacunae (seen under the light microscope) is not empty but filled by a different material. It is likely that the 'dark globule' is located deeper within this material. This material was further analyzed by EDS analysis (see next section).

SEM-EDS chemical analysis of the intralacunar material of brown bones

EDS is a technique for elemental analysis, but it can directly indicate the most probable mineral found in the sample based on its elemental composition. SEM-EDS shows that the intralacunar material are embedded within a fossilized bone matrix made of fluorapatite (as shown by the presence of fluorine (F), indicating that the original hydroxyapatite was converted to fluorapatite (Data S1 to S3)). EDS analysis performed on the intralacunar material directly revealed the widespread presence of phosphorus and calcium, but the concentration of the elements is not the same in all lacunae, and even varies within the same lacuna (Fig. 7). Beside from phosphorus, four other different types of elements are characteristics of the intralacunar material: aluminum (Al), calcium

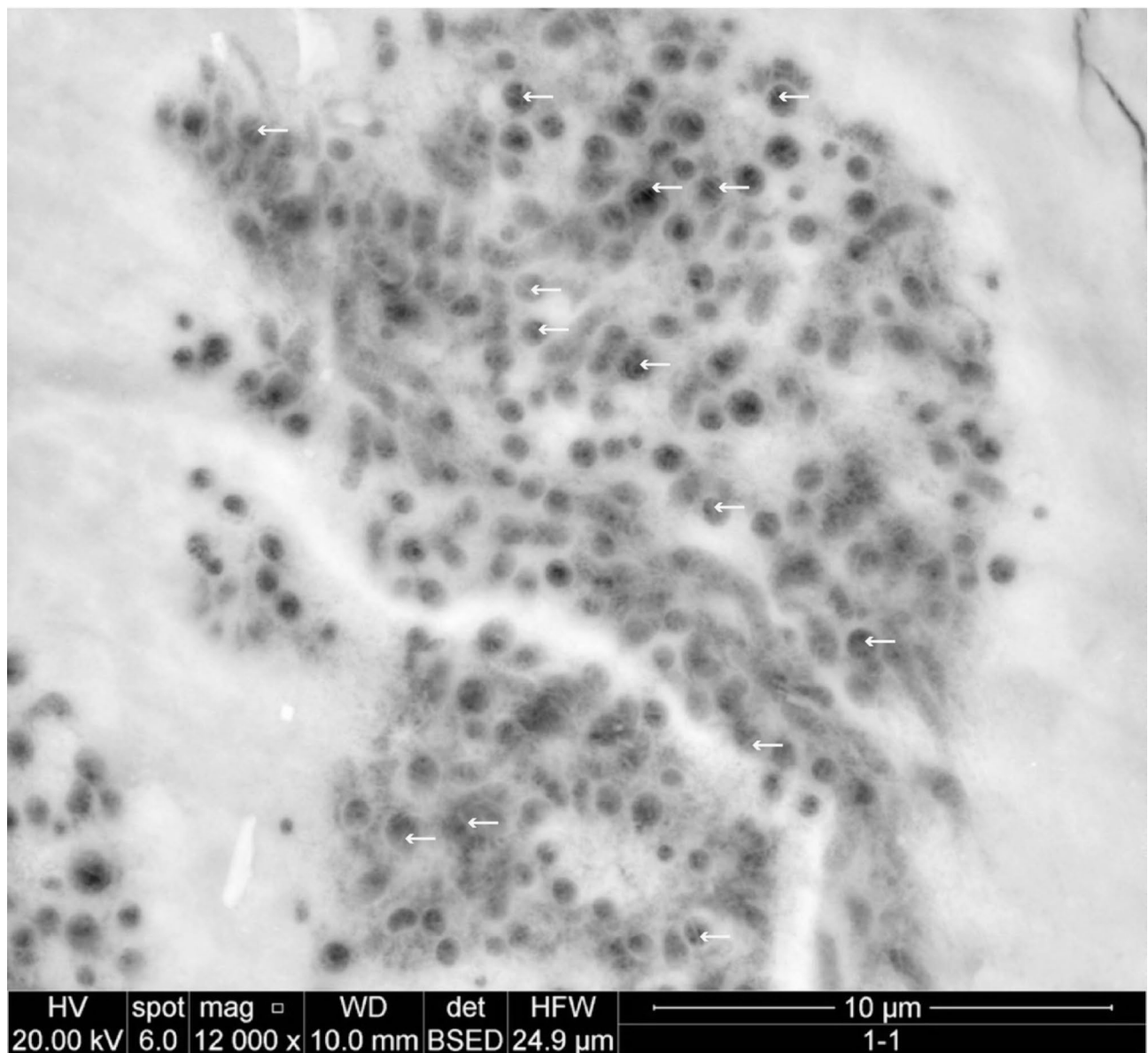


Fig. 3. SEM image of pores and channels made by a bacterial colony in QU-1, with fibrous material within the pores. The white arrows indicate the fibrous material in the pores.

(Ca), silicon (Si) and iron (Fe) respectively (Fig. 7C-E). They also present some carbon (C) and oxygen (O) (Fig. 7 and see full EDS raw data into Data S4-6).

Decalcification results

To further investigate the potential presence of cells within this material from the DAM1 fossil site, we decalcified two additional patellae. EDTA decalcification has proven useful to reveal cellular fossilization in many fossils^{29,30,32–35}. After decalcification of a brown patella (QU-8) in EDTA for 4 days, the bony matrix revealed the presence of many chondrocyte-like structures, osteocyte-like structures, and blood vessel-like structures (Fig. 8A-D). They are consistent in morphology with cells and soft tissues found in previous studies of fossil samples and that of extant mammals^{29,30,32–35}. These structures were not observed in the white QU-7 after 4 days in decalcifying solution (Fig. S5).

After 11 days in EDTA (with no solution change), one small drop of solution from the decalcified brown QU-8 was filled in a much higher concentration of these osteocyte-like structures, blood vessel-like structures, and some pieces of bony matrix with cell-like structures still attached to it (Fig. 8F, H). All of these structures were brown in color (Fig. 8). These decalcified products are very different from those of the white patella QU-7 after 11 days in EDTA: they show no cell-like structures, only broken blood vessel-like structures, and a few pieces of altered bone matrix (Fig. 8E, G).

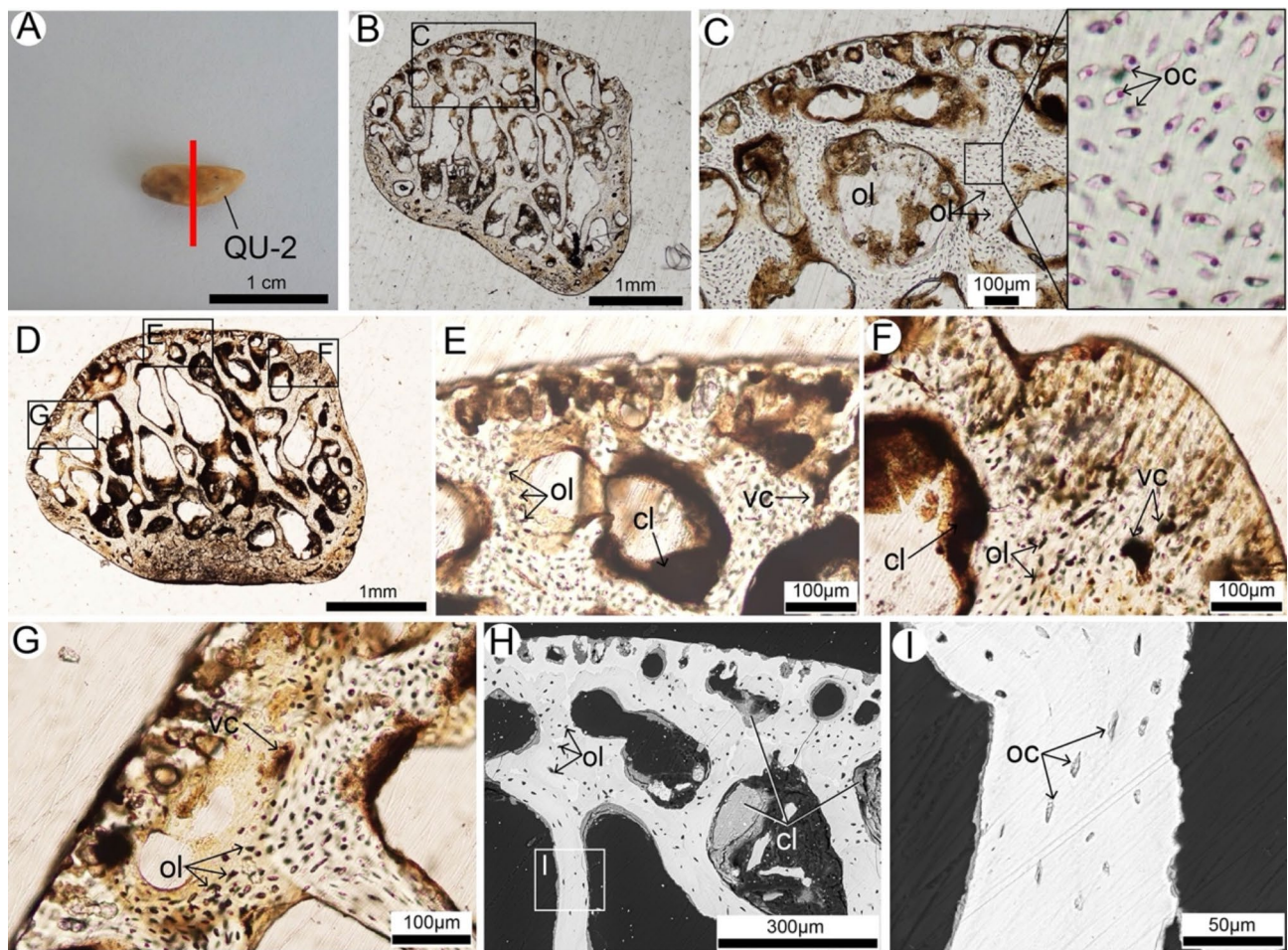


Fig. 4. Histology of the brown patella QU-2. **A**, photograph of the patella QU-2 with the red line indicating the direction of the section; **B**, histological of slice one of QU-2 under transmitted light and its close-up (**C**), showing the unaltered bone tissue and the intralacunar preservation; **D**, histological of slice two of QU-2 under transmitted light and its close-up (**E-G**); **H**, corresponding SEM image of (**E**) and its close-up (**I**), showing the infilled osteocyte lacuna; These brown bone shows pristine histological preservation and no bacterial invasion. **cl**, chondrocyte lacuna; **oc**, osteocyte; **ol**, osteocyte lacuna; **vc**, vascular canal.

Discussion

The histological investigations in six bones of the site DAM1 revealed that the white bones were completely bacterially invaded (Figs. 2, 5B-C and 6C), whereas the brown and beige bones were not (Figs. 4, 5D-I and 6E). In the bacterially invaded white bones, the SEM clearly revealed well-defined bacterial erosions that decreased the bone matrix density (Fig. 2E, F). Bone matrix density decrease is commonly observed during bacterial invasions (e.g., during taphonomic experiments on extant bone³⁶ or in other vertebrate fossils, such as fossils from the Miocene of Northwest China^{31,37}). Bacteria dissolve the bone matrix and make it spongier during their invasion^{38–40}. Sometimes a brighter hypermineralized rim can form around the colonies and corresponds to a redeposition of bone minerals^{28,37,40} but such a hypermineralized rim was not visible in any of the samples analyzed here.

EDTA decalcification of the brown patella QU-8 showed that it was completely filled with chondrocyte-like, osteocyte-like and blood vessel-like structures, themselves also brown in color (Fig. 8A, F, H). On the other hand, the decalcified white patella QU-7 showed no cell-like structures at all and only a few pieces of broken blood vessel-like structures (that looked partially consumed by bacteria) and broken pieces of bony matrix (Fig. 8E, G). From all of the data combined together (i.e., histological, SEM and decalcification results), it appears that the bacterial colonies found within the white bones consumed the original organic matter and structures. One logical conclusion to make is that the brown color of the bones (QU-2, QU-4; QU-5, QU-8 and the diaphysis of QU-6) is due to the presence of organic matter/soft tissue structures and cells. Somehow these brown bones must have been shielded from bacterial attacks, because all the white bones analyzed here are full of bioerosions and show no cells and only soft tissues that are consumed by bacteria (Fig. 8G). The data does not support that these structures are casts⁴¹ but rather original endogenous structures that were not eaten by bacteria in the brown bones, and remnants of endogenous structures that are partially consumed by bacteria in the white bones.

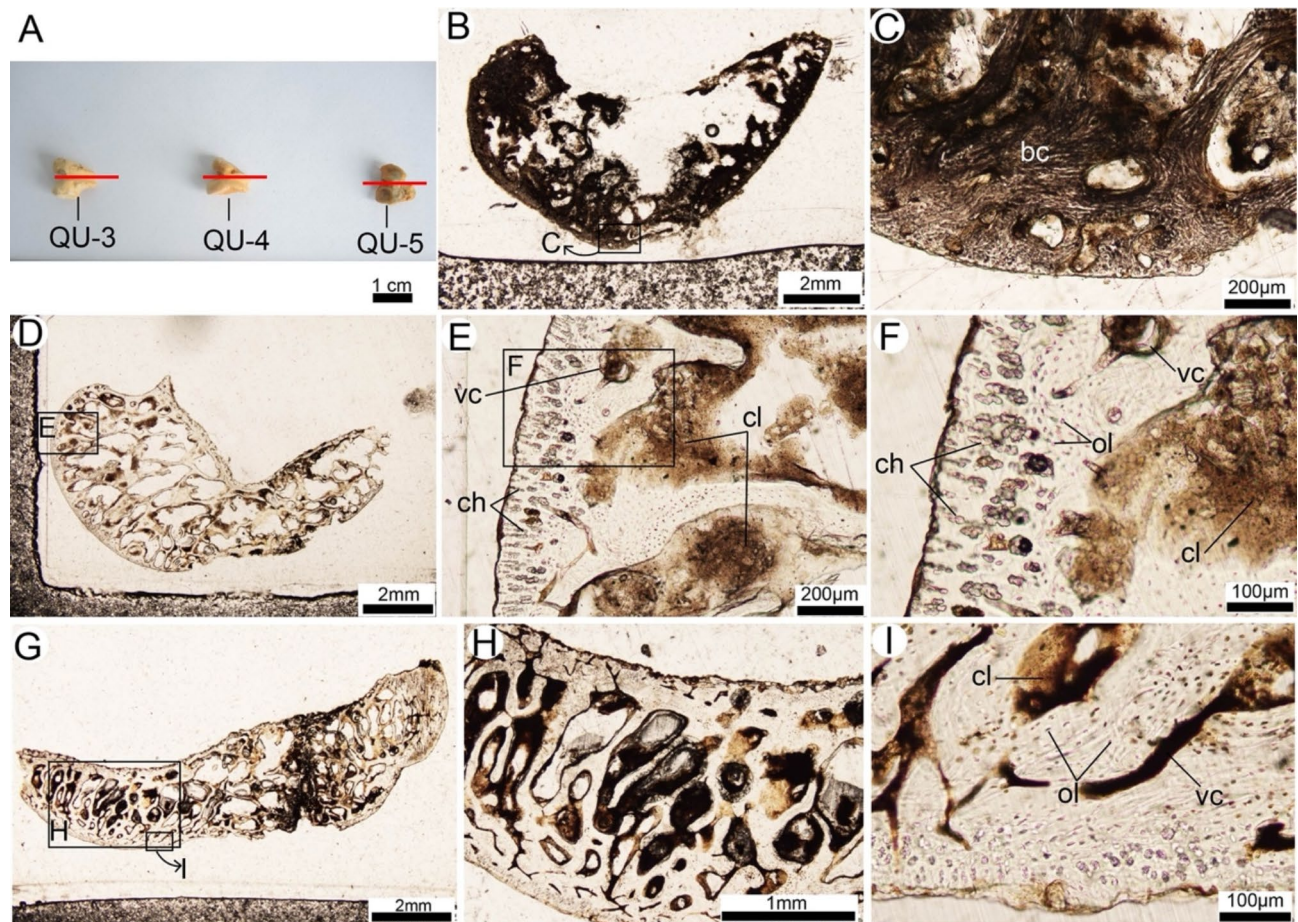


Fig. 5. Histology of three distal femoral heads (unfused) ranging from white (QU-3), to beige (QU-4) and to brown (QU-5). **A**, photograph of QU-3 to 5 with red line indicate the direction of section; **B**, histological of ground section slice of QU-3 under transmitted light and its close-up (**C**), showing the bacterial colonies as in the white patella QU-1; **D**, histological of ground section slice of QU-4 under transmitted light and its close-up (**E-F**); **G**, histological of ground section slice of QU-5 under transmitted light and its close-up (**H-I**); **D-I** show the unaltered bone and well preserved bone matrix as in the brown patella QU-2. Thickness of slide B, D and G is 89 microns, 98 microns and 95 microns respectively. bc, bacterial colony; ch, chondrocyte lacuna; cl, clay; ol, osteocyte lacuna; vc, vascular canal.

This is supported by the results of another study on Cretaceous-Paleogene vertebrates preserved in glauconitic greensands⁴². In this study, the fossil specimens that were dark in color exhibited excellent microscopic bone preservation and yielded a greater recovery of original soft tissues, whereas light-colored specimens exhibited poor microscopic preservation and yielded few to no soft tissues. This paper even discussed that the color variation in these bones was likely caused by microbial degradation⁴². The histological images provided in this paper do show a bone that looks invaded by microorganisms⁴². The present paper therefore represents another example of study that suggest bacterial invasions and bone color are linked. In parallel, it is also possible that an enrichment in iron oxides in the samples analyzed here (e.g., Fig. 6F) altered the original (non-fossilized) colors of all the microstructures analyzed here (i.e., bone, osteocyte-like and chondrocyte-like structures, blood vessel-like structures) into a brown color. Iron oxides have been proposed to help preserve soft tissues and cells in deep time, in some instances^{32,33}.

Bioerosion is a common determinant of bone preservation and can give insights on the early post-mortem history^{40,43}. In our study, bioerosion was found in all white fossil bones of DAM1, but not in the brown bones. Since not all of the bones analyzed here were bacterially invaded, it means something stopped the bacteria from growing at some point after burial. The bones are not obviously rounded, indicating that they have not been transported over long distances. The intensity and distribution of bacterial colonies in the specimens suggest soil attack as in the bones from Neuad³⁶: bacterial colonies appear scattered and dispersed, not associated with vascular supply, and/or peripherally affecting the periosteal and endosteal cortical layers (Fig. S1-S2), leaving the medial cortical layer almost unaffected³⁶. Therefore, it is possible that the microenvironments of these fossils in the early stages of burial were different.

Our interpretation is that, in DAM1, the bones that were attacked by bacteria remained on the surface of the sediment for some time in an environment that was probably saturated with water, conditions that allowed the

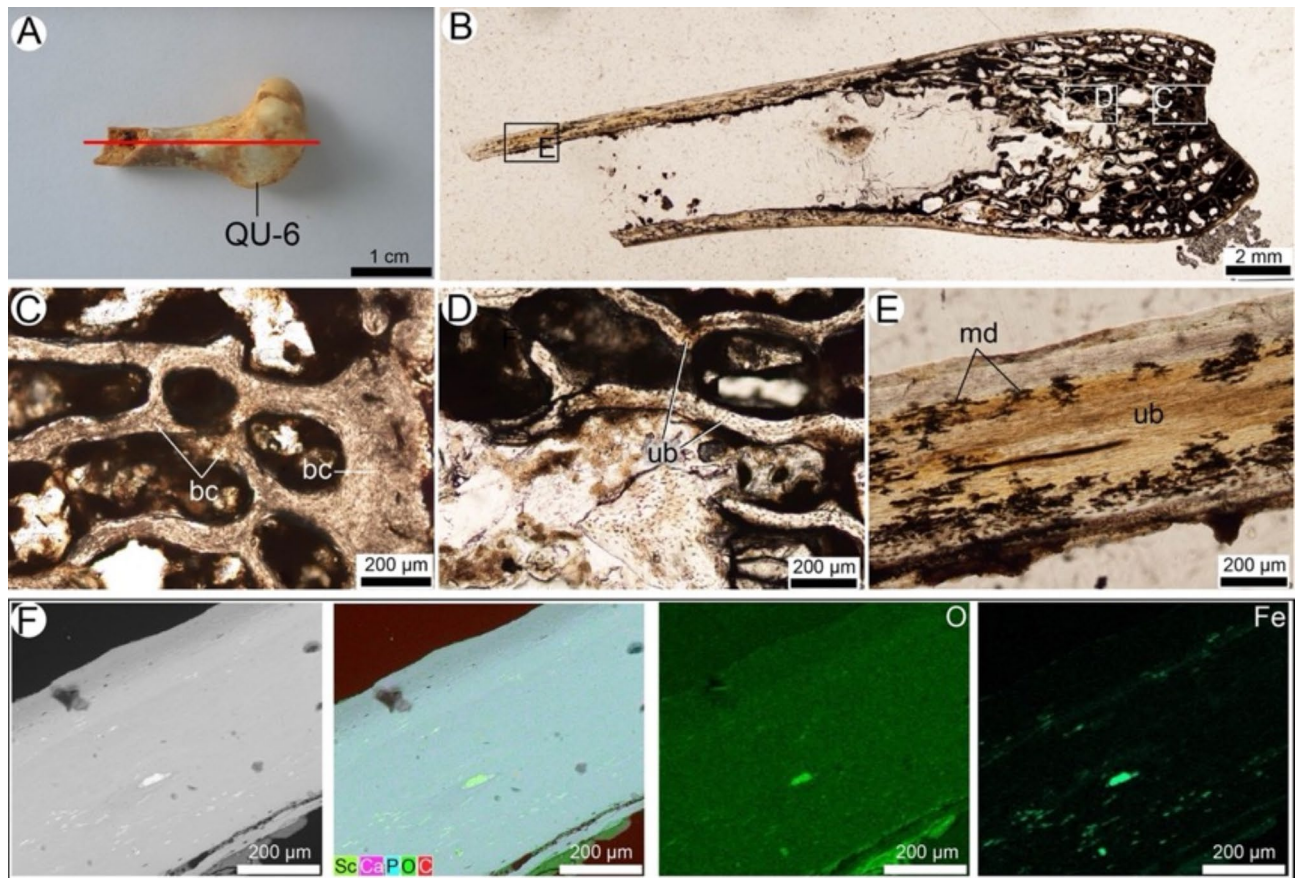


Fig. 6. Histology of a distal femur (QU-6) with brown diaphysis and white epiphysis. **A**, photograph of QU-6 with red line indicate the direction of section; **B**, histological of ground section slice of QU-6 under transmitted light and its close-up of epiphysis (**C**), metaphysis (**D**) and diaphysis (**E**), showing the bacterial colonies in the epiphysis as in the white patella QU-1, and unaltered bone in the metaphysis and diaphysis as in the brown patella QU-2; **F**, EDS of (**E**) showing the iron deposition in the bone matrix. Slide thickness is 120 microns. bc, bacterial colony; md, mineral deposition; ub, unaltered bone.

bacteria to attack the bones directly. At the same time, other bones may have been buried in the detritic sediment -certainly saturated with water. This detritic sediment directly or indirectly filled the bone porosity. Indirectly, this means that chemical attack on the detrital sediment provided the chemical elements that made up the various mineral phases that precipitated and/or accumulated in the porosity, in particular within the osteocyte lacunae (see next section).

It is the first time that bacterial invasions are reported and histologically analyzed in any fossil of the Quercy phosphorites, giving an interesting insight on the taphonomy of the newly discovered site of DAM1 and showing that fossils in the Quercy are not always exceptionally preserved. It is however too difficult to tell when exactly the invasions occurred after death, nor how long they were going on until the death of all the bacterial colonies, but it is plausible to hypothesize attacks occurred during early diagenesis rather than during late diagenesis.

After just four days into a decalcifying solution, the brown patella QU-8 released many isolated osteocytes with very clear canaliculi, chondrocytes and blood vessels (Fig. 8). After 11 days in this same solution, the solution was replete with cells and blood vessels (Fig. 8). Light microscopy revealed dark clay and ferruginous sediments in the trabecular gaps and in the vascular channels of another brown patella (QU-2); in this same patella structures resembling cells with a globular nucleus were seen (QU-2; Fig. 4C). This type of fine preservation was expected due to the fine preservation potential of phosphatization^{18–20}. We focused the EDS beams on these same structures and found that they are composed of aluminum, silicon, calcium, phosphorus, and iron, which most likely indicate the presence of at least partly authigenic minerals in the the osteocyte lacunae like silica, calcium phosphate, clay and probably goethite (Figs. 4I and 7). These structures also contained some carbon and oxygen (Fig. 7; Data S4–S6). All of the evidence taken together suggests that the intralacunar content seen under the light microscope (Fig. 4C) and under the SEM (Fig. 7) are fossilized cells (like those seen in Fig. 8). Additionally, although EDS is elemental, the EDS results suggest that the bones that were not invaded by bacteria have cells that were mineralized by various mineralized phases, including calcium phosphate, alumino-silicates, carbonates, silica and iron oxides (Fig. 7). This has also been observed in other fossilized osteocytes^{30,31}. For example, alumino-silicified, silicified, and ironized chondrocytes were reported in *Yanornis*, *Confuciusornis*, and *Caudipteryx* from the Early Cretaceous Jehol biota of China^{32,44} and ironized osteocytes were found in non-

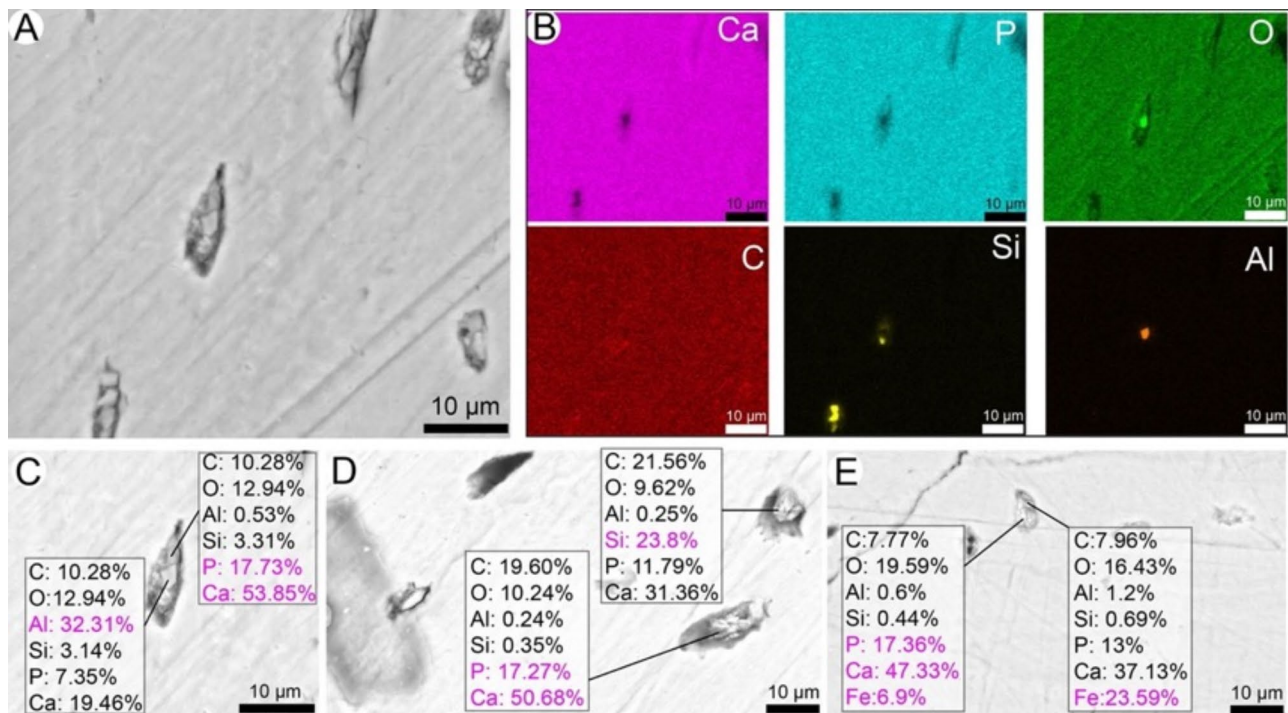


Fig. 7. EDS analysis of the intralacunar content in brown QU-2. **A**, close up SEM image of the osteocyte lacunae in Fig. 4I and EDS analysis on the same image (**B**), showing the different chemical element content of the different lacunae and different location in the same lacuna; Alumino-silicified (Abundant Si and Al, probably component of clay) (**C**), calcified (Abundant Ca and P, probably components of hydroxyapatite or fluoroapatite) (**C-D**), silicified (Abundant Si, probably a component of Silica) (**D**). Another analysis in a brown part of QU-6 (in the diaphysis) shows ironized intralacunar content (**E**).

avian dinosaurs from Late Cretaceous of North America³³. Ironized osteocytes-like structures were found in *Mongolemys* from the Late Cretaceous of Mongolia³⁰. Cases of calcified fossil cells are relatively less reported, such as that of a royal fern from the Early Jurassic of Sweden⁴⁵. Similarly to what is observed in this current study, different types of mineralization occurred in cells within the same specimen of *Caudipteryx* and *Mongolemys*, further supporting that having a different mineralogical composition in different cells within one same fossil is not a rare phenomenon at all^{30,32}. It is also important to note that some cell lacunae are highly likely also filled with ‘pollution’ rather than in-situ mineralization.

As a famous phosphate mine, it is logical for the Quercy to be a favorable environment to preserve fossil cells. Fine structures preserved by phosphatization require a rapid replacement of the structures by mineral deposition⁴⁶, which is consistent with our observation of rapid burial for the DAM1 specimens in situ. In the present study, phosphorous was present- but was only one of the elements identified in the DAM1 fossilized osteocytes and intralacunar structures (Fig. 7). Phosphate is also favorable to subcellular preservation such as nuclei preservation (e.g²⁵). Further histochemical work is necessary to test whether or not the globules within the cells seen under the light microscope (Fig. 4C) are indeed remnants of cell nuclei. A similar type of cellular preservation with fossilized nuclei has already been observed in previous studies in fossils of all ages and from all around the world⁴⁷. In fact, cell nuclei appear to be quite common in the fossil record with some recently discovered examples in the Cretaceous dinosaur *Hypacrosaurus* from Montana or a Jurassic Royal fern from Sweden^{45,48}. In vertebrates, cartilage seems to be a good tissue for cellular and nuclear preservation (e.g⁴⁸), and chondrocytes in calcified cartilage are supposed to be more resistant to autolysis in general than osteocytes⁴⁹. Although chondrocytes were not well visible in the ground-section slices of the brown specimens studied here, the decalcification method did help the identification of plenty of fossilized chondrocytes in the brown patella QU-8 (Fig. 4J-M). This highlights the importance of applying more than one method for the detection of different cellular structures and/or tissues within one same sample. Our decalcification method showed that chondrocytes are indeed preserved here in at least some specimens of DAM1 and suggests future histochemical and cellular analyses on DAM1 cartilage are necessary.

Studies suggest that microbial activity may have a positive impact on the mineralization and on the preservation of organic matter through the crystallization of microbial biofilms on the decomposing organic matter⁵⁰. Studies also suggest the metabolic products of bacterial decay generate the conditions promoting precipitation^{19,51}. Previous research suggests that phosphate in bones may be the source of phosphorus for Quercy phosphorylation². Bacterial decomposition may release phosphorus from the bones into the surrounding groundwater, providing a source of phosphorus for mineralization¹⁹. Here, our results do not support these interpretations for the specific site of DAM1, it appears that instead, bacterial invasions (which apparently

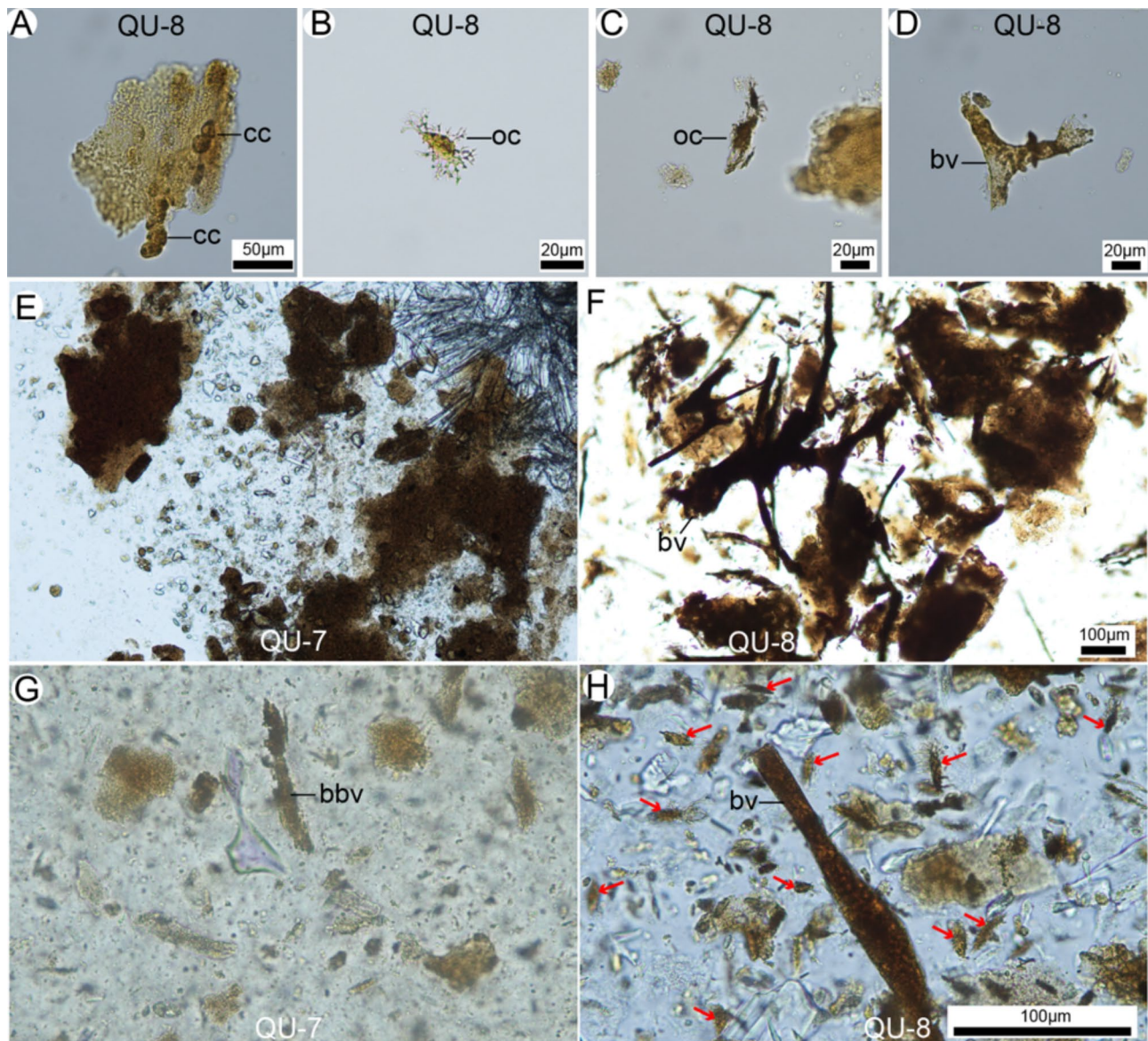


Fig. 8. Microphotographs of decalcified contents of white patella QU-7 and brown patella QU-8. Decalcified contents of QU-8 after 4 days in EDTA (A-D). Decalcified contents of white patella QU-7 after 11 days in EDTA in (E) and (G). Decalcified content of brown QU-8 after 11 days in EDTA in (F) and (H). Images E and F have the same scale. Images G and H have the same scale. In QU-7, the ‘broken blood vessel’ (bbv) is clearly eaten away (G); the red arrows in (H) are pointing at osteocytes in QU-8. bv, blood vessel; cc, chondrocyte; oc, osteocyte.

occurred early during burial rather than later during diagenesis) limited the preservation of organic matter (i.e., blood vessels, and cells) in the bones of DAM1. The Quercy is highly likely filled with unique taphonomies at each of its sites, even perhaps between two sites very close to each other and this requires further attention.

Conclusion and future research

Our results show that the different colors of the Cainotheriidae from DAM1 are linked with different fossilization conditions, bioerosions, and most likely the presence of organic matter. The light-colored fossils experienced obvious bioerosions, while the dark-colored fossils did not and preserved fine microstructures including fossilized osteocytes. These skeletal tissues with cellular fossilization might have undergone a very different taphonomic and diagenetic process from the exceptionally 3D-preserved fossils with soft tissues in the Quercy. Here, the identification of cellular structures as an endogenous cellular preservation relies on histology, SEM-EDS analyses, and decalcification. Histochemical and immunohistochemical analyses contributed to the identification of fossil cells in diverse other taxa^{33,52–54}. Future investigations should include more robust histochemical and molecular analyses directly on isolated osteocytes that are released after EDTA decalcification to test for the presence of fossil cell nuclei at the chemical level and to better understand the overall chemistry

of the cells. In depth-mineralogical studies will also be necessary to better understand the full context of their preservation and surrounding bone chemistry. These rigorous examinations are essential for a comprehensive understanding of these specimens and additional Quercy bones. Additionally, a recent study shows the 3D preserved phosphatized fossil of Quercy also preserve bones, but the soft tissues were hypothesized to be casts⁹. It is unlikely that the soft tissues are simply casts and future investigations should delve into comparing the preservation of bones preserved with and without soft tissues, and to better understand the preservation of soft-tissues and cells themselves.

Materials and methods

Site DAM1

The studied osteological material comes from the karstic locality of Dams (near Caylus SW France), specifically from the DAM1 channel discovered in 2016⁷. This cavity, partially emptied during 19th -century intensive phosphate mining, still houses a large quantity of clay infillings and preserves several fossiliferous infillings of different ages. In particular, two fossiliferous channels, DAM1 and DAM2, yielded an impressive number of well-preserved Cainotheriid remains due to low-energy transport⁷. Biochronological dating suggests an MP19 age (late Priabonian; ca. 34.1 My) for DAM1 and DAM2 infillings, based on rodent assemblages.

The Quercy phosphate infilling sites in SW France comprise over 200 localities recording local faunal assemblages with a temporal resolution of approximately 1 million years or less, covering a time span of more than 30 million years^{55–57}. This unique area shelters abundant fossiliferous caves with a continuous record spanning the 42–24 Ma interval (late middle Eocene–late Oligocene), capturing a dynamic history and significant global climatic changes.

Paroxacron valdense MP19 Upper Eocene

The fossil material examined in this study belongs to a small artiodactyl family, the Cainotheriidae, specifically identified as *Paroxacron valdense*⁷. This species represents over 90% of the fossil assemblage of both DAM1 and DAM2 localities. Cainotheriids are small artiodactyls known from the late Eocene to the middle Miocene in Western Europe^{7,58,59}. This family is rather well diversified and is composed of around twenty species for at least six genera^{58,59}. Cainotheriid remains are particularly abundant in the fossil record and notably in karstic infillings from the phosphorites of the Quercy^{7,57–59}. Two isolated patellae (UM-DAM1-278, -279), three distal femoral epiphyses (UM-DAM1-280 to -282), and a broken distal part of a femur (UM-DAM1-283) were selected for histological analysis in this research, because they were thought to possess both bone and calcified cartilage. Two additional patellae were decalcified in EDTA (UM-DAM1-285, -286). For readability, we assigned shorter numbers (QU-1 to 8) for these specimens used in this study (Table S1).

Histology

The specimens were embedded in EXAKT Technovit 7200 resin and cured for 12 h, cut into slices (Figs. 2, 3, 4, 5 and 6, see the red lines) and polished until the desired optical contrast was reached. Ground sections were observed under transmitted and polarized light using a Nikon Eclipse LV100NPOL and photographed with a DS-Fi3 camera and the software NIS-Element v4.60.

SEM-EDS

The ground sections were analyzed at the Chinese Academy of Geological Sciences (Beijing) using FEI Quanta 450 (FEG) at 20 kV. Both BSE and SE modes (back-scattered electrons and secondary electrons) were applied to the ground-sections. Both elemental mapping and specific points were targeted. Slides were un-coated.

EDTA decalcification

QU-7 and QU-8 (Fig. 7) were decalcified in a solution of EDTA (0.5 M; pH 8.0) for 11 days (without any solution change). Two microscopic analyses were made, one after four days in EDTA, and then a second one after 11 days. For photography, one drop of solution is pipetted on top of a glass slide which is then cover-slipped. These slides need to be rapidly photographed before evaporation.

Data availability

The data that support the findings of this study are available from the corresponding author upon reasonable request.

Received: 25 March 2024; Accepted: 25 September 2024

Published online: 10 October 2024

References

1. Rage, J. C. The lower vertebrates from the Eocene and Oligocene of the Phosphorites du Quercy (France): An overview. (2006).
2. Schwermann, A. et al. The fossil insects of the Quercy region: A historical review. *Entomol. Heute.* **28**, 127–142 (2016).
3. Peigné, S. A new species of *Eofelis* (Carnivora: Nimravidae) from the phosphorites of Quercy, France. *C. R. Acad. Sci. Ser. IIA Earth Planet. Sci.* **330**, 653–658 (2000).
4. D Bonis, L. Ursidae (Mammalia, Carnivora) from the late oligocene of the Phosphorites Du Quercy (France) and a reappraisal of the genus Cephalogale Geoffroy, 1862. *Geodiversitas.* **35**, 787–814 (2012).
5. de Bonis, L., Gardin, A. & Blondel, C. Carnivora from the early oligocene of the ‘Phosphorites Du Quercy’ in southwestern France. *Geodiversitas.* **41**, 601–621 (2019).
6. Solé, F. et al. The upper eocene-oligocene carnivorous mammals from the Quercy phosphorites (France) housed in Belgian collections. *Geol. Belg.* **24** (2020).

7. Weppe, R. et al. Cainotheriidae (Mammalia, Artiodactyla) from dams (Quercy, SW France): Phylogenetic relationships and evolution around the eocene–oligocene transition (MP19–MP21). *J. Syst. Palaeontol.* **18**, 541–572 (2020).
8. Laloy, F. et al. A re-interpretation of the Eocene anuran *Thaumastosaurus* based on microCT examination of a ‘mummified’ specimen. *PLOS ONE*. **8**, e74874 (2013).
9. Tissier, J. et al. Synchrotron analysis of a ‘mummified’ salamander (Vertebrata: Caudata) from the Eocene of Quercy, France. *Zool. J. Linn. Soc.* **177**, 147–164 (2016).
10. Tissier, J., Rage, J. C. & Laurin, M. Exceptional soft tissues preservation in a mummified frog-eating Eocene salamander. *PeerJ*. **5**, e3861 (2017).
11. van de Kamp, T. et al. Parasitoid biology preserved in mineralized fossils. *Nat. Commun.* **9**, 3325 (2018).
12. Georgalis, G. L., Čerňanský, A. & Klembař, J. Osteological atlas of new lizards from the Phosphorites Du Quercy (France), based on historical, forgotten, fossil material. *Geodiversitas*. **43**, 219–293 (2021).
13. Legendre, S. et al. Les phosphorites Du Quercy: 30 ans de recherche. Bilan et perspectives. *Geobios*. **30**, 331–345 (1997).
14. Billaud, Y. Les paragénèses phosphatées du paléokarst des phosphorites du Quercy. (1982).
15. Cavagnetto, C. & Anadón, P. Preliminary palynological data on floristic and climatic changes during the Middle Eocene-Early Oligocene of the eastern Ebro Basin, northeast Spain. *Rev. Palaeobot. Palynol.* **92**, 281–305 (1996).
16. Akhmetiev, M. A. & Beniamovski, V. N. Paleogene floral assemblages around epicontinental seas and straits in Northern Central Eurasia: proxies for climatic and paleogeographic evolution. *Geologica Acta*. **7**, 297–309 (2009).
17. Orr, P. J. Late proterozoic–early phanerozoic ‘taphonomic windows’: the environmental and temporal distribution of recurrent modes of exceptional preservation. *Paleontol. Soc. Pap.* **20**, 289–313 (2014).
18. Schiffbauer, J. D., Wallace, A. F., Broce, J. & Xiao, S. Exceptional fossil conservation through phosphatization. *Paleontol. Soc. Pap.* **20**, 59–82 (2014).
19. Briggs, D. E. G., Kear, A. J., Martill, D. M. & Wilby, P. R. Phosphatization of soft-tissue in experiments and fossils. *J. Geol. Soc.* **150**, 1035–1038 (1993).
20. Wilson, P., Parry, L. A., Vinther, J. & Edgecombe, G. D. Unveiling biases in soft-tissue phosphatization: Extensive preservation of musculature in the cretaceous (cenomanian) polychaete *Rollinschaeta myoplena* (Annelida: Amphinomidae). *Palaeontology*. **59**, 463–479 (2016).
21. Chen, J. Y. et al. Precambrian animal diversity: putative phosphatized embryos from the Doushantuo Formation of China. *Proc. Natl. Acad. Sci.* **97**, 4457–4462 (2000).
22. Xiao, S. & Knoll, A. H. Phosphatized animal embryos from the neoproterozoic doushantuo formation at Weng'an, Guizhou, South China. *J. Paleontol.* **74**, 767–788 (2000).
23. Yin, L. et al. Doushantuo embryos preserved inside diapause egg cysts. *Nature*. **446**, 661–663 (2007).
24. Martill, D. M. Macromolecular resolution of fossilized muscle tissue from an elopomorph fish. *Nature*. **346**, 171–172 (1990).
25. Parry, L. A. et al. Soft-bodied fossils are not simply rotten carcasses – Toward a holistic understanding of exceptional fossil preservation. *BioEssays*. **40**, 1700167 (2018).
26. McNamara, M. E. et al. Reconstructing carotenoid-based and structural coloration in fossil skin. *Curr. Biol.* **26**, 1075–1082 (2016).
27. Hackett, C. J. Microscopical focal destruction (tunnels) in exhumed human bones. *Med. Sci. Law*. **21**, 243–265 (1981).
28. Turner-Walker, G. Light at the end of the tunnels? The origins of microbial bioerosion in mineralised collagen. *Palaeogeogr. Palaeoclimatol. Palaeoecol.* **529**, 24–38 (2019).
29. Hall, B. K. *Bones and Cartilage: Developmental and Evolutionary Skeletal Biology* (Elsevier/Academic, 2005).
30. Cadena, E. A. In situ SEM/EDS compositional characterization of osteocytes and blood vessels in fossil and extant turtles on untreated bone surfaces: Different preservational pathways microns away. *PeerJ*. **8**, e9833 (2020).
31. Li, Z., Bailleul, A. M., Stidham, T. A., Min, W. & Tao, D. Exceptional preservation of an extinct ostrich from the late Miocene Linxia Basin of China. *Vertebr. Palasiat.* **59**, 229–244 (2021).
32. Zheng, X., Bailleul, A. M., Li, Z., Wang, X. & Zhou, Z. Nuclear preservation in the cartilage of the Jehol dinosaur *Caudipteryx*. *Commun. Biol.* **4**, 1125 (2021).
33. Schweitzer, M. H. et al. A role for iron and oxygen chemistry in preserving soft tissues, cells and molecules from deep time. *Proc. R. Soc. B Biol. Sci.* **281**, 20132741 (2014).
34. Schweitzer, M. H. Soft tissue preservation in terrestrial mesozoic vertebrates. *Annu. Rev. Earth Planet. Sci.* **39**, 187–216 (2011).
35. Ullmann, P. V., Pandya, S. H. & Nellermoe, R. Patterns of soft tissue and cellular preservation in relation to fossil bone tissue structure and overburden depth at the Standing Rock Hadrosaur Site, Maastrichtian Hell Creek formation, South Dakota, USA. *Cretac. Res.* **99**, 1–13 (2019).
36. Fernández-Jalvo, Y. et al. Early bone diagenesis in temperate environments: Part I: Surface features and histology. *Palaeogeogr. Palaeoclimatol. Palaeoecol.* **288**, 62–81 (2010).
37. Turner-Walker, G. Early bioerosion in skeletal tissues: Persistence through deep time. *Neues Jahrb. Geol. Paläontol. - Abh.* **265**, 165–183 (2012).
38. Jackes, M., Sherburne, R., Lubell, D., Barker, C. & Wayman, M. Destruction of microstructure in archaeological bone: A case study from Portugal. *Int. J. Osteoarchaeol.* **11**, 415–432 (2001).
39. Turner-Walker, G., Nielsen-Marsh, C. M., Syversen, U., Kars, H. & Collins, M. J. Sub-micron spongiform porosity is the major ultra-structural alteration occurring in archaeological bone. *Int. J. Osteoarchaeol.* **12**, 407–414 (2002).
40. Jans, M. M. E. Microbial bioerosion of bone – A review. In *Current Developments in Bioerosion* (eds Wissak, M. & Tapanila, L.). 397–413. https://doi.org/10.1007/978-3-540-77598-0_20 (Springer, 2008).
41. Kaye, T. G., Gaugler, G. & Sawlowicz, Z. Dinosaurian soft tissues interpreted as bacterial biofilms. *PLoS ONE*. **3**, e2808 (2008).
42. Voegele, K. K. et al. Soft tissue and biomolecular preservation in vertebrate fossils from glauconitic, shallow marine sediments of the Hornerstown formation, Edelman Fossil Park, New Jersey. *Biology*. **11**, 1161 (2022).
43. Smith, C. I., Nielsen-Marsh, C. M., Jans, M. M. E. & Collins, M. J. Bone diagenesis in the European holocene I: Patterns and mechanisms. *J. Archaeol. Sci.* **34**, 1485–1493 (2007).
44. Bailleul, A. M. & Zhou, Z. SEM analyses of fossilized chondrocytes in the extinct birds *Yanornis* and *confuciusornis*: Insights on taphonomy and modes of preservation in the Jehol Biota. *Front. Earth Sci.* **9**, 718588 (2021).
45. Bomfleur, B., McLoughlin, S. & Vajda, V. Fossilized nuclei and chromosomes reveal 180 million years of genomic stasis in royal ferns. *Science*. **343**, 1376–1377 (2014).
46. Briggs, D. E. The role of decay and mineralization in the preservation of soft-bodied fossils. *Annu. Rev. Earth Planet. Sci.* **31**, 275 (2003).
47. Bailleul, A. M. Fossilized cell nuclei are not that rare: review of the histological evidence in the Phanerozoic. *Earth-Sci. Rev.* **216**, 103599 (2021).
48. Bailleul, A. M. et al. Evidence of proteins, chromosomes and chemical markers of DNA in exceptionally preserved dinosaur cartilage. *Natl. Sci. Rev.* **7**, 815–822 (2020).
49. Bailleul, A. M., Wu, Q., Li, D., Li, Z. & Zhou, Z. Do chondrocytes within calcified cartilage have a higher preservation potential than osteocytes? A preliminary taphonomy experiment. *Vertebr. Palasiat.* **61**, 108 (2023).
50. Peterson, J. E., Lenczewski, M. E. & Scherer, R. P. Influence of microbial biofilms on the preservation of primary soft tissue in fossil and extant archosaurs. *PLOS ONE*. **5**, e13334 (2010).
51. Briggs, D. E. G. & Kear, A. J. Fossilization of soft tissue in the laboratory. *Science*. **259**, 1439–1442 (1993).

52. Pawlicki, R. Histochemical demonstration of DNA in osteocytes from dinosaur bones. *Folia Histochem. Cytophisiol.* **33**, 183–186 (1995).
53. Bailleul, A. M. & Li, Z. DNA staining in fossil cells beyond the Quaternary: reassessment of the evidence and prospects for an improved understanding of DNA preservation in deep time. *Earth-Sci. Rev.* **216**, 103600 (2021).
54. Wu, Q., Bailleul, A. M. & Li, Z. H. Application of paraffin section and histochemistry technique in paleohistology of fossil samples. *Bio* **101** (2021).
55. Aguilar, J. P., Legendre, S. & Michaux, J. Biochronologie mammalienne du cénozoïque en Europe et domaines reliés. In *Actes du Congrès BiochroM'97* (1997).
56. Escarguel, G., Legendre, S. & Sigé, B. Unearthing deep-time biodiversity changes: The Palaeogene mammalian metacommunity of the Quercy and Limagne area (Massif Central, France). *C. R. Geosci.* **340**, 602–614 (2008).
57. Weppe, R., Orliac, M. J., Guinot, G. & Condamine, F. L. Evolutionary drivers, morphological evolution and diversity dynamics of a surviving mammal clade: Cainotherioids at the eocene–oligocene transition. *Proc. R Soc. B Biol. Sci.* **288**, 20210173 (2021).
58. Blondel, C. New data on the Cainotheriidae (Mammalia, Artiodactyla) from the early oligocene of south-western France. *Zool. J. Linn. Soc.* **144**, 145–166 (2005).
59. Weppe, R., Blondel, C., Vianey-Liaud, M., Pélassié, T. & Orliac, M. J. A new Cainotherioidea (Mammalia, Artiodactyla) from Palembert (Quercy, SW France): phylogenetic relationships and evolutionary history of the dental pattern of Cainotheriidae. *Palaeontol. Electron.* <https://doi.org/10.26879/1081> (2020).

Acknowledgements

We thank Zhang Shukang and Zhu Yuxia for preparing the ground section slices. We thank Maeva Orliac at the ISEM (Institut des Sciences de l'Évolution de Montpellier) for providing all of the samples for this study and for discussions. This work was supported by the Youth Innovation Promotion Association Grant of the Chinese Academy of Sciences (2023078) and National Natural Science Foundation of China NSFC grant 42350610256 to AMB. NSFC grant 42302012 and the Beijing Natural Science Foundation (5224037) supported QW. The collection of study material in the field was financially supported by the ANR DEADENDER and ENLIVEN programs (grants ANR-18-CE02-0003-01 and ANR-22-CE02-0014-01) - PI Mr J. Orliac and the association "Phosphatières du Quercy".

Author contributions

A. M. B designed the project. Q. W. and A. M. B collected the data. Q. W., R. W., C. L., Y. P., A. M. B analyzed the data and wrote the paper.

Declarations

Competing interests

The authors declare no competing interests.

Additional information

Supplementary Information The online version contains supplementary material available at <https://doi.org/10.1038/s41598-024-74301-y>.

Correspondence and requests for materials should be addressed to Q.W. or A.M.B.

Reprints and permissions information is available at www.nature.com/reprints.

Publisher's note Springer Nature remains neutral with regard to jurisdictional claims in published maps and institutional affiliations.

Open Access This article is licensed under a Creative Commons Attribution-NonCommercial-NoDerivatives 4.0 International License, which permits any non-commercial use, sharing, distribution and reproduction in any medium or format, as long as you give appropriate credit to the original author(s) and the source, provide a link to the Creative Commons licence, and indicate if you modified the licensed material. You do not have permission under this licence to share adapted material derived from this article or parts of it. The images or other third party material in this article are included in the article's Creative Commons licence, unless indicated otherwise in a credit line to the material. If material is not included in the article's Creative Commons licence and your intended use is not permitted by statutory regulation or exceeds the permitted use, you will need to obtain permission directly from the copyright holder. To view a copy of this licence, visit <http://creativecommons.org/licenses/by-nc-nd/4.0/>.

© The Author(s) 2024